iopscience.iop.org

Home Search Collections Journals About Contact us My IOPscience

An analytic estimate of the maximum Lyapunov exponent in products of tridiagonal random matrices

This article has been downloaded from IOPscience. Please scroll down to see the full text article.

1999 J. Phys. A: Math. Gen. 32 7603

(http://iopscience.iop.org/0305-4470/32/44/301)

View the table of contents for this issue, or go to the journal homepage for more

Download details:
IP Address: 171.66.16.111
The article was downloaded on 02/06/2010 at 07:48

Please note that terms and conditions apply.

J. Phys. A: Math. Gen. **32** (1999) 7603–7621. Printed in the UK PII: S0305-4470(99)05445-1

An analytic estimate of the maximum Lyapunov exponent in products of tridiagonal random matrices

F Cecconi†§ and A Politi‡‖

† Dipartimento di Fisica, Università di Firenze, Firenze, Italy
‡ Istituto Nazionale di Ottica, Firenze, Italy

Received 24 June 1999

Abstract. In this work we present a theoretical and numerical study of the behaviour of the maximum Lyapunov exponent in products of random tridiagonal matrices in the limit of small coupling and small fluctuations. Such a problem is directly motivated by the investigation of coupled-map lattices in a regime where the chaotic properties are quite robust and yet a complete understanding has still not been reached. We derive some approximate analytic expressions by introducing a suitable continuous-time formulation of the evolution equation. As a first result, we show that the perturbation of the Lyapunov exponent due to the coupling depends only on a single scaling parameter which, in the case of strictly positive multipliers, is the ratio of the coupling strength with the variance of local multipliers. An explicit expression for the Lyapunov exponent is obtained by mapping the original problem onto a chain of nonlinear Langevin equations, which are eventually reduced to a single stochastic equation. The probability distribution of this dynamical equation provides an excellent description for the behaviour of the Lyapunov exponent. Finally, multipliers with random signs are also considered, finding that the Lyapunov exponent again depends on a single scaling parameter, which, however, has a different expression.

1. Introduction

Coupled-map lattices (CMLs) represent an interesting class of models for the investigation of several spatio-temporal phenomena, ranging from pattern formation to synchronization and spatio-temporal chaos. Even though the discreteness of both space and time variables makes CMLs more amenable to numerical simulations than partial differential equations, the development of analytical techniques remains a difficult task. As usual, when dealing with difficult problems, it is convenient to start from the identification of some relatively simple limit and thereby develop a perturbative approach. In the case of lattice dynamics, there are two opposite limits that are worth investigation: the weak- and strong-coupling regimes. In the former case, one can use all the knowledge acquired about low-dimensional systems to predict the dynamical properties when spatial directions are added. In this spirit, general theorems have been formulated and proved about both the structure of the invariant measure [1] and the existence of travelling localized excitations [2]. The weak-coupling limit is also interesting in connection with the synchronization of chaotic attractors, a problem that can be studied effectively by looking at the behaviour of the Lyapunov exponents [3]. In the opposite limit, one expects a slow spatial dependence and, correspondingly, the existence of a few, dynamically

§ Also with INFN Sezione di Firenze.
‖ Also with INFN Unita' di Firenze.

0305-4470/99/447603+19$30.00 © 1999 IOP Publishing Ltd

active, degrees of freedom. This is the spirit that has led to the study of different truncations of partial differential equations.

The maximum Lyapunov exponent (MLE) is one of the most useful indicators of chaos; it is, therefore, desirable to provide a possibly analytic description of its dependence on the coupling strength as well as on the local chaotic properties. The first author who investigated the effect of a small coupling on chaotic dynamics was Daido [4], who numerically studied two coupled maps as well as two continuous-time chaotic oscillators. He also made an attempt to combine analytical considerations with numerical studies to explain the observed behaviour, without, however, being able to go beyond the prediction of the scaling behaviour.

In fact, the problem, in its entirety, is already rather nontrivial in the weak-coupling limit, since various factors concur to modify the chaotic properties of the dynamics: (i) perturbation of the invariant measure; (ii) the onset of spatial correlations in real space; (iii) the onset of correlations in tangent space. The last phenomenon is the most interesting one for at least two reasons: first, it leads to counterintuitive effects such as an increase of the MLE even in the presence of a stabilizing coupling; second, it provides the leading contribution in the weak-coupling limit. It is precisely because of its presence that the power-law dependence described in [5] for some CML model only extends over a finite range of coupling strengths [6].

In order to be more precise, let us introduce a standard CML model,

$$\begin{aligned} x_i(t+1) &= f(y_i(t+1)) \\ y_i(t+1) &= \varepsilon x_{i-1}(t) + (1-2\varepsilon)x_i(t) + \varepsilon x_{i+1}(t) \end{aligned} \qquad (1)$$

where the $x_i(t)$ represents the state variable in the site i at time t, $y_i(t)$ is an auxiliary dummy variable, and ε represents the coupling strength. The function $f(y)$ is a map of the interval with chaotic properties (e.g. the logistic function $4y(1-y)$) and, finally, periodic boundary conditions are assumed. An infinitesimal perturbation $u_i(t)$ satisfies the following evolution rule:

$$u_i(t+1) = m_i(t)\{\varepsilon u_{i-1}(t) + (1-2\varepsilon)u_i(t) + \varepsilon u_{i+1}(t)\} \qquad (2)$$

where $m_i(t) \equiv f'(y_i(t+1))$ is the so-called local multiplier. In practice, one should determine $f'(y_i(t+1))$ from the evolution in real space, i.e. from equation (1) (this step involves the first two of the above-mentioned factors) and thereby derive the dynamical properties of the perturbation field.

Both to facilitate a theoretical analysis and because a previous study has shown that the first two factors are less important [7], we shall introduce a random-matrix approximation, assuming that $m_i(t)$ is a given δ-correlated stochastic process,

$$\langle m_j(\tau) m_i(t)\rangle = D\delta_{i,j}\delta_{t,\tau}. \qquad (3)$$

In fact, random-matrix approximations have proven to be very effective in various dynamical systems [8–10].

In spite of the simplifications introduced by neglecting spatial (and temporal) correlations, not even the scaling behaviour of the MLE has been completely clarified. Indeed, the approaches implemented in some previous papers [7, 11] have not been able to go beyond a qualitative explanation of the dependence on the coupling strength. Here, instead, we aim at presenting a fully quantitative, though approximate, treatment for the MLE in the small-coupling regime. We restrict our analysis to the usual diffusive coupling scheme defined in equation (2), but we are confident that the present approach can be effectively adapted to different (short-range) interaction schemes.

The first approach [7] devised to deal with the random-matrix process (2) exploited the analogy with the statistical mechanics of directed polymers in random media. Indeed, equation (2) can be also read as the recursive equation for the partition function '$u_i(t)$' of a polymer of length t which grows by adding any new monomer no farther than one site from the last one. A possibly relevant difference between the two problems comes from the 'Boltzmann weight' m_i which is necessarily positive in the polymer case (being a probability), while it can be negative in a CML (by recalling the interpretation of m_i as the derivative of the map f). This is the first issue that makes treatment of problem (2) more difficult and it is the reason why previous studies have been restricted to the case of strictly positive multipliers [7, 11]. In fact, without entering the mathematical treatment, one can see that if m_i can be either positive or negative, $u_i(t)$ is no longer positive definite and partial cancellations can occur in the iteration of the recursive relation.

The efforts made in [7] to estimate the MLE consisted of developing a mean-field analysis on the basis of the equivalence between the MLE and the free energy in directed polymers. Thus, by using the approaches developed in [12, 13], it was possible to show that the spatial coupling induces an increase of the MLE from the 'quenched' average $\Lambda_0 = \langle \log m_i \rangle$ (corresponding to the absence of a spatial coupling) towards the 'annealed' average $\Lambda_0 = \ln\langle m_i \rangle$ that holds above some critical coupling value. While some features of this scenario were qualitatively confirmed by the numerical simulations (as, e.g., the increase of the MLE), no evidence of the phase transition was actually found. A perturbative technique, developed later on to improve the previous estimates [11] has shown that the transition point slowly shifts towards larger coupling values, possibly disappearing in the asymptotic limit. Nevertheless, the extremely slow convergence of the estimates of the MLE to the values numerically observed, makes a general implementation of this approach unappealing. Moreover, we should also recall that the analogy with directed polymers does not even allow an exact prediction of the scaling behaviour of the MLE, insofar as it indicates the existence of an additional, extremely weak, dependence on the coupling strength which seems to be absent in the outcome of direct numerical simulations.

It is also worth recalling the analogy between the behaviour of the MLE and the evolution of rough interfaces. By interpreting the logarithm of (the amplitude of) the perturbation as the height of an abstract interface, the Lyapunov exponent becomes equivalent to the velocity of one such interface [14, 15]. However, this analogy is of no utility in the present case, since the deviation of the MLE from the uncoupled limit cannot be determined by studying the corresponding Kardar–Parisi–Zhang (KPZ) equation as already remarked in [11]. In a sense, the MLE corrections are connected to non-trivial deviations from a KPZ behaviour over short temporal and spatial scales.

In this paper we derive approximate but analytical expression for the MLE, by mapping the original dynamics onto to a chain of continuous-time, nonlinear Langevin equations. Such a set of equations is then reduced to a single stochastic equation whose solution yields an expression for the MLE that is in good agreement with direct numerical simulations. As the whole approach does not make use of the specific structure of the initial equations, we are rather confident that it can be repeated for other types of couplings, and presumably the only difference will be the structure of the deterministic force in the final stochastic equation. Moreover, we would like to point out that the mapping onto continuous-time equations indicates that the initial discreteness of the time variable is not a distinctive feature and we can imagine that a similar approach also works in the case of coupled chaotic oscillators. Our hope is reinforced by the observation that some equations obtained in the present framework can also be derived in the case of two weakly coupled differential equations [16].

The paper is organized as follows. In section 2, we briefly introduce the problem and some notations. In section 3 we discuss the properties of tangent dynamics in the case of strictly positive multipliers: the analytical treatment is followed by a comparison with the numerical results. In section 4 we extend the analytical treatment to the case of multipliers with random signs. Finally, in section 5 we summarize the main results and comment about the problems still open. The two appendices are devoted to the small-noise limit in the case of strictly positive multipliers and, respectively, to the small-coupling regime in the general case of random signs.

2. Preliminary treatment

In this section, we formulate the problem of computing the MLE under the assumption of a small-coupling strength. The first step consists of introducing the ratio between the perturbation amplitude in two consecutive sites,

$$R_j(t) \equiv u_j(t)/u_{j-1}(t) \tag{4}$$

which allows one to write equation (2) as

$$\ln\left|\frac{u_i(t+1)}{u_i(t)}\right| = \ln|m_i(t)| + \ln\left|1 - 2\varepsilon + \varepsilon R_{i+1}(t) + \frac{\varepsilon}{R_i(t)}\right| \tag{5}$$

where the average of the lhs is nothing but the MLE $\Lambda(\varepsilon)$, while the rhs is naturally expressed as the sum of the zero-coupling value plus the correction term induced by spatial interactions.

A more convenient way of writing the Lyapunov exponent is obtained by transforming the smallness parameter as

$$\gamma \equiv \varepsilon/(1 - 2\varepsilon) \tag{6}$$

which leads to

$$\Lambda(\varepsilon) = \left\langle \ln\left|\frac{u_i(t+1)}{u_i(t)}\right|\right\rangle = \Lambda(0) + \ln(1 - 2\varepsilon) + \delta\Lambda(\gamma) \tag{7}$$

where the Lyapunov correction is split into two parts, a multiplier-independent term and a non-trivial contribution

$$\delta\Lambda(\gamma) = \left\langle \ln\left|1 + \gamma R_{i+1} + \frac{\gamma}{R_i}\right|\right\rangle \tag{8}$$

where $\langle\cdot\rangle$ represents the time average along the trajectory generated by equation (1) or, equivalently, the ensemble average if ergodicity holds.

Equation (8) tells us that the determination of the MLE requires the prior knowledge of the invariant measure of the stochastic process $R_i(t)$ on two consecutive sites. By expanding the logarithm in powers of γ, the correction to the MLE can be expressed in terms of all the momenta of the probability distribution,

$$\delta\Lambda(\gamma) = -\sum_{j=1}^{\infty}\sum_{m=1}^{j} \frac{(j-1)!(-\gamma)^j}{m!(j-m)!}\langle R_{i+1}^m R_i^{j-m}\rangle. \tag{9}$$

It is, therefore, quite useful to derive a dynamical equation for $R_i(t)$. Let us start by rewriting the tangent dynamics in the two consecutive sites $\{i-1, i\}$ in terms of the R_i variables

$$\frac{u_{i-1}(t+1)}{u_{i-1}(t)} = m_{i-1}(t)\{1 - 2\varepsilon + \varepsilon/R_{i-1}(t) + \varepsilon R_i(t)\}$$

$$\frac{u_i(t+1)}{u_i(t)} = m_i(t)\{1 - 2\varepsilon + \varepsilon/R_i(t) + \varepsilon R_{i+1}(t)\}.$$

By taking the ratio between these two equations we find, after some rearrangements,

$$R_i(t+1) = \mu_i(t) R_i(t) \frac{1 + \gamma R_{i+1}(t) + \gamma/R_i(t)}{1 + \gamma R_i(t) + \gamma/R_{i-1}(t)} \tag{10}$$

where we have introduced the stochastic process

$$\mu_i(t) \equiv m_i(t)/m_{i-1}(t) \tag{11}$$

whose geometric average is equal to one, μ_i being the ratio of two i.i.d. processes.

3. Positive multipliers

We first consider strictly positive multipliers, while the more general case is addressed in the following section. In fact, while the two cases require a somewhat different treatment, a discussion of the former problem allows the introduction of several tools that turn out to be also useful in the latter context.

3.1. Theory

If the μ_i are positive definite, the ratios R_i remain positive whenever initialized as such. This allows one to introduce the variable $w_i = \ln R_i$ without having to deal with the sign of R_i. The introduction of w_i is convenient in that it transforms the original problem into a stochastic process with additive rather than multiplicative noise. With no restriction other than the positiveness of the multipliers, we obtain

$$w_i(t+1) - w_i(t) = \ln \mu_i(t) + \ln\{1 + \gamma \mathrm{e}^{w_{i+1}(t)} + \gamma \mathrm{e}^{-w_i(t)}\} - \ln\{1 + \gamma \mathrm{e}^{w_i(t)} + \gamma \mathrm{e}^{-w_{i-1}(t)}\}. \quad (12)$$

In the small-γ limit we can expand the logarithms and retain only the leading linear terms in γ†,

$$w_i(t+1) - w_i(t) = -2\gamma \sinh(w_i) + \gamma(\mathrm{e}^{w_{i+1}} - \mathrm{e}^{-w_{i-1}}) + \xi_i(t) \quad (13)$$

where $\xi_i \equiv \ln \mu_i$ is a stochastic process with zero average and correlation function,

$$\langle \xi_i(t)\xi_j(t')\rangle = 4\sigma^2 \delta_{t,t'}(\delta_{i,j} - \tfrac{1}{2}\delta_{i\pm1,j}) \quad (14)$$

where σ^2 is the variance of the logarithm of m_i and the factor 4 replaces the usual factor 2, since the noise term is the ‘sum’ of two i.i.d. processes ($\xi_i = \ln m_i - \ln m_{i-1}$). The spatial correlations between neighbouring sites, i, $i+1$ follow from the very definition of ξ_i: the process $\ln m_i$ enters the definition of both ξ_i and ξ_{i+1}.

The smallness of γ in equation (13) makes it possible to interpret the lhs of such an equation as a time derivative, $w_i(t+1) - w_i(t) \sim \dot{w}_i(t)$, provided that the noise term ξ_i is not large as well, and thus to write a continuous-time stochastic differential equation

$$\dot{w}_i = -2\gamma \sinh(w_i) + \gamma(\mathrm{e}^{w_{i+1}} - \mathrm{e}^{-w_{i-1}}) + \xi_i(t). \quad (15)$$

The correctness of the above conclusion (and the accuracy of the approximations) can be controlled by deriving the corresponding Fokker–Planck equation from the original integral equation for the the probability distribution $P_L(w_1, \ldots, w_L; t)$ for the discrete-time dynamics (13). As the calculations are conceptually straightforward and lead to the result that one would expect from the Langevin equation (15), we limit ourselves to recall the key step: because of the smallness of the noise fluctuations, the convolution with the probability distribution of the stochastic force can be transformed into differential calculus by expanding P_L up to the second derivative. As a result, one finds the Fokker–Planck equation

$$\frac{\partial P_L}{\partial t} = -\sum_{i=1}^{L} \frac{\partial}{\partial w_i}\{F(w_i)P_L + \Phi(w_{i+1}, w_{i-1})P_L\} + \frac{1}{2}\sum_{i,j=1}^{L} \mathcal{D}_{i,j} \frac{\partial^2 P_L}{\partial w_i \partial w_j} \quad (16)$$

where

$$F(w_i) = -2\gamma \sinh(w_i) \quad (17)$$

is the single-particle force (see equation (15)), $\Phi(w_{i+1}, w_{i-1}) = -2\gamma(\mathrm{e}^{w_{i+1}} - \mathrm{e}^{-w_{i-1}})$ is the coupling term and $\mathcal{D}_{i,j}$ are the diffusion coefficients obtainable from (14).

† A rigorous justification of this approximation can be obtained *a posteriori*, once we have seen that $\langle \gamma \exp(\pm w_i)\rangle \to 0$ for $\gamma \to 0$.

Equation (15) represents a chain of coupled Langevin equations describing the evolution of interacting 'particles'. Even without solving the model, it is possible to realize that a single parameter suffices to describe the scaling behaviour of the Lyapunov exponent, the rescaled smallness parameter

$$g = \gamma/\sigma^2 \tag{18}$$

which can also be interpreted as the inverse effective diffusion constant. In fact, the factor γ in front of the deterministic forces can be eliminated by properly scaling the time units.

In section 3.2, we numerically investigate the validity of this prediction, by plotting the Lyapunov exponent (obtained for different values of σ, γ and two choices of the probability distribution of multipliers) versus g: a data collapse onto a single curve will represent the direct confirmation that g is the only relevant parameter.

The evaluation of $\delta\Lambda(\gamma)$ requires finding the invariant measure for the whole set of stochastic equations (15). This is still a difficult problem, since the deterministic forces do not follow from a potential and, therefore, the corresponding Fokker–Planck equation cannot be straightforwardly solved. In particular, it is interesting to notice that, although we are working in the limit of weakly coupled maps, the 'particles' are not weakly interacting. This is the most serious difficulty when performing a perturbative treatment of the problem. The only strategy that we have found to obtain a meaningful analytic estimate of the Lyapunov exponent is a mean-field approach. It allows reducing the, in principle, infinite set of stochastic equations to a single effective Langevin equation. In spite of the unavoidable approximation, we shall see that the resulting analytic expression is reasonably close to the numerical results.

Let us now introduce the single-particle distribution $P(w_i)$, by integrating over all the other $L-1$ degrees of freedom

$$P(w_i, t) = \int \prod_{j \neq i} \mathrm{d}w_j \, P_L(w_1, \ldots, w_L; t).$$

The corresponding equation can be directly derived from equation (16),

$$\frac{\partial P}{\partial t} = -\frac{\partial}{\partial w_i}\{F(w_i)P\} + 2\sigma^2 \frac{\partial^2 P}{\partial w_i^2} - \gamma \frac{\partial}{\partial w_i}\left\{ \int \mathrm{d}w_{i+1} \, P_2(w_i, w_{i+1}) \mathrm{e}^{w_{i+1}} - \int \mathrm{d}w_{i-1} \, P_2(w_{i-1}, w_i) \mathrm{e}^{-w_{i-1}} \right\}. \tag{19}$$

Equation (19) is not closed since it involves the unknown two-body distribution P_2. Indeed, the above equation is the first of a hierarchy of equations involving probability distributions of increasing order. The simplest approximation to close the system consists of truncating the hierarchy at the lowest level by assuming a perfect factorization, $P_2(x, y) = P(x)P(y)$. This is the standard mean-field approach which leads to the closed Fokker–Planck equation

$$\frac{\partial P}{\partial t} = -\frac{\partial}{\partial w}\{F(w)P\} + 2\sigma^2 \frac{\partial^2 P}{\partial w^2} \tag{20}$$

since the symmetry of the distribution ($P(w) = P(-w)$) implies that the coupling terms cancel each other.

The Fokker–Planck equation (20) corresponds to the single-particle Langevin equation

$$\dot{w} = F(w) + \xi(t) \tag{21}$$

where we have dropped the by now irrelevant spatial dependence.

It is instructive to test the validity of the above approximation in the limit of large g values, when the forces can be linearized and an analytic solution can be obtained for the entire chain of Langevin equations. For the sake of readability, the discussion of this technical problem is presented separately in the first appendix. The main result of this analysis is that the approximation (21) is exact! The stationary probability distribution of equation (20) is equal to the projection of the many-particle distribution for the whole chain. However, one cannot expect that the same also holds true for finite g values, when nonlinearities come into play.

The stationary distribution w is obtained by solving the Fokker–Planck equation (20),

$$P(w) = \mathcal{C} \exp[-\gamma/\sigma^2 \cosh(w)] \tag{22}$$

where the normalization constant $\mathcal{C} = 2K_0(\gamma/\sigma^2)$ is expressed in terms of the zeroth-order modified Bessel function [17, 18]

$$K_\nu(x) = \int_{-\infty}^{\infty} \mathrm{d}t \; \exp\{-x \cosh(t) \pm \nu t\}.$$

By substituting the definition of w ($w = \ln R$) in equation (9), and assuming $\langle w_i w_{i-1} \rangle = 0$ (an hypothesis accurately confirmed by direct numerical simulations), we finally obtain

$$\delta\Lambda(\gamma) = -\sum_{j=1}^{\infty} \sum_{m=1}^{j} \frac{(j-1)!(-\gamma)^j}{m!(j-m)!} \frac{K_m(2g)K_{j-m}(2g)}{K_0(2g)^2}. \tag{23}$$

As γ is assumed to be small, we can safely retain only the first two terms of the series (23), obtaining

$$\delta\Lambda(\gamma) = 2\gamma \; \frac{K_1(2g)}{K_0(2g)} \tag{24}$$

which represents the (approximate) perturbative expression for the correction to the MLE in the limit of small coupling.

First of all, it is instructive to investigate the limit $g \ll 1$, by using the asymptotic expression of the functions $K_\nu(y)$. Since

$$K_0(y) \sim -\ln(y/2) \qquad K_1(y) \sim \frac{1}{y} \tag{25}$$

we find that

$$\delta\Lambda(\gamma) \sim \frac{\sigma^2}{\ln(1/g)}. \tag{26}$$

This equation represents a relevant improvement over the previous results. First of all, it is in agreement with numerical simulations which do not give evidence of a $\ln|\ln g|$ correction in the numerator, as instead predicted by the statistical-mechanics treatment based on the analogy with directed polymers [11].

A second and more important remark concerns the dependence on the 'noise' strength which is explicitly determined. Previously, it was only clear that the correction to the MLE must vanish if there is no multifractality (no multiplier fluctuations) but the dependence on σ was not known.

3.2. Numerical results

The theoretical analysis performed in the previous section is based mainly on a perturbative approach. Moreover, it involves a nontrivial transformation of a set of coupled Langevin equations to a single effective Langevin equation in a limit where the coupling is not negligible. Therefore, a comparison of the theoretical predictions with direct numerical simulations is especially worthwile to check the validity of the dynamical mean-field approximation that is behind this last step.

We have decided to test the theoretical results by using two different probability densities: (A) uniform distribution of multipliers m_i within the interval $[e^a(1-\Delta_1/2), e^a(1+\Delta_1/2)]$; (B) uniform distribution of the logarithms of the m_i within $[a-\Delta_2/2, a+\Delta_2/2]$. The corresponding Lyapunov exponents in the uncoupled limit ($\varepsilon = 0$) are

$$\Lambda_A(0) = a - 1 + \frac{1}{\Delta_1}\left\{\left(1+\frac{\Delta_1}{2}\right)\ln\left(1+\frac{\Delta_1}{2}\right) - \left(1-\frac{\Delta_1}{2}\right)\ln\left(1-\frac{\Delta_1}{2}\right)\right\} \qquad \Lambda_B(0) = a$$

while the variances of $\ln m_i(t)$ are

$$\sigma_A^2 = 1 - \frac{1}{\Delta_1^2}\left(1-\frac{\Delta_1^2}{4}\right)\ln^2\left(\frac{1+\Delta_1/2}{1-\Delta_1/2}\right) \tag{27}$$

$$\sigma_B^2 = \frac{\Delta_2^2}{12}. \tag{28}$$

We start by testing the predictions for the shape of the probability distribution of w. Two meaningful examples are reported in figure 1, where the open circles refer to the histograms, while the solid curves are the theoretical results. Let us first comment about the qualitative shape of the distribution. In the limit of large g, the noise is almost negligible and therefore, the phase point is not expected to deviate significantly from the stable fixed point $w = 0$. It is therefore possible to linearize the equation, finding a Gaussian distribution. This is precisely the message contained in figure 1(*a*), which refers to $g = 2.4$. Alternatively, in the limit of small g, it is the force that can be neglected except when the deviations are large. Since the attracting force grows very rapidly (exponentially), it makes sense to replace the corresponding potential with a flat well with infinitely high barriers placed where the deterministic force is of the same order as the stochastic one. In this picture, one expects that the probability distribution is just a uniform distribution in a finite interval (this is the kind of argument introduced in [7] to predict the scaling behaviour in this regime). This scenario can be qualitatively recognized in figure 1(*b*), which refers to $g = 0.021$.

Next, let us comment on the quantitative agreement between the theoretical expectations and the numerical findings. In figure 1(*a*), there is an almost perfect agreement. However, some deviations are observed in figure 1(*b*), where the theoretical curve is slightly more peaked. A better agreement is obtained if the scaling parameter g is taken as a free parameter to be fitted (see the dashed curve in figure 1(*b*) which corresponds to a 20% smaller value of g than expected). The same scenario is observed for all other parameter values, the deviation from the theoretical expectation always being smaller than 30%. These results suggest that the model (21) could be improved by renormalizing the coupling constant γ. Some preliminary results confirm this perspective [19].

Since the aim of the present paper is to study the corrections to the MLE induced by the spatial coupling, let us now discuss this issue. In order to assess the quality of our theoretical predictions, we performed numerical iterations of equation (2) computing the MLE with the well known algorithm presented in [20]. Simulations have been carried out on 500-site lattices, imposing periodic boundary conditions. In every simulation the first 500 iterations have been discarded to avoid any bias effect due to initial conditions. Tests made with different lattice lengths indicate that finite-size effects are always much smaller than the deviation from the theoretical predictions.

The first nice result is provided by figure 2(*a*). The data is plotted in order to emphasize the existence of a single relevant parameter, g. Indeed, the good data collapse (all data align along the same curve irrespective of the value of γ, σ or the type of probability distribution) represents a further confirmation of our theoretical analysis. Moreover, the nice agreement of the numerical data with the theoretical expression (24) (see the solid curve in figure 2(*a*)) over

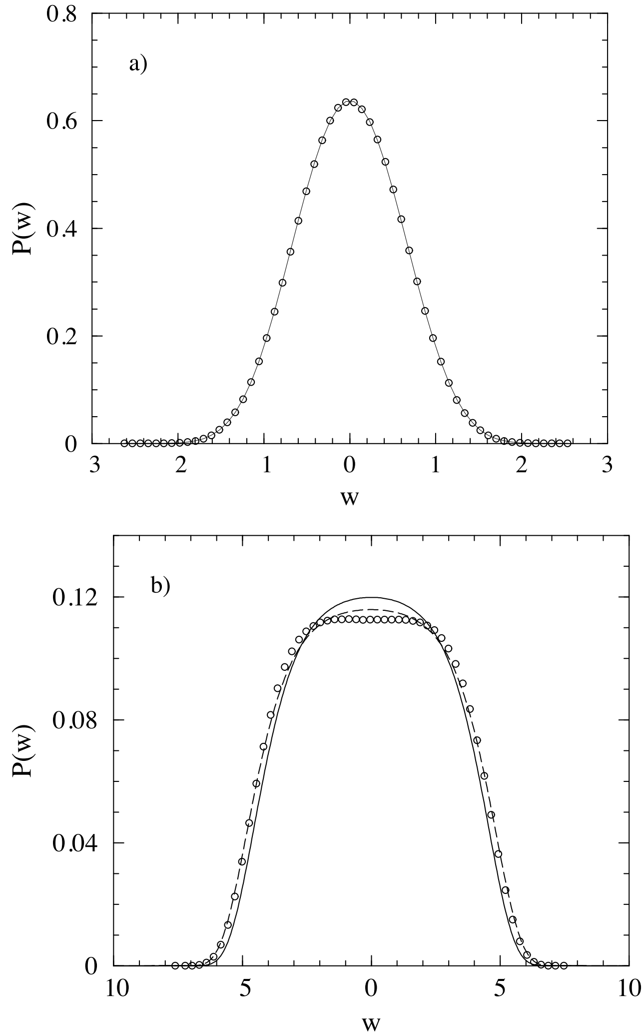

Figure 1. The probability distribution of w for two different values of g: 2.4 (*a*) and 0.021 (*b*). In both cases, circles refer to the numerical histograms, obtained by iterating equation (2) for 5×10^7 time steps (discarding the first 10^3 iterations) on a lattice of $L = 300$ sites. The solid curves correspond to the analytic formula (equation (22)). The dashed curve in (*b*) is obtained by fitting g, which is estimated to be equal to 0.016.

a wide range of values of the effective coupling testifies to the accuracy of the approximations introduced in the first part of this section.

However, there is a better way to emphasize the differences between theory and numerics. In fact, the limit $g \to \infty$ corresponds to negligible noise, i.e. to a regime where the MLE Lyapunov exponent is unaffected by the presence of spatial coupling as shown in [21]. It is therefore convenient to look at the behaviour of the whole deviation of the Lyapunov exponent $\Delta\Lambda = \delta\Lambda - 2\gamma$, which again exhibits the same scaling behaviour, as seen by dividing this expression by σ^2 and using equation (26):

$$\frac{\Delta\Lambda}{\sigma^2} = 2g\left(\frac{K_1(2g)}{K_0(2g)} - 1\right). \tag{29}$$

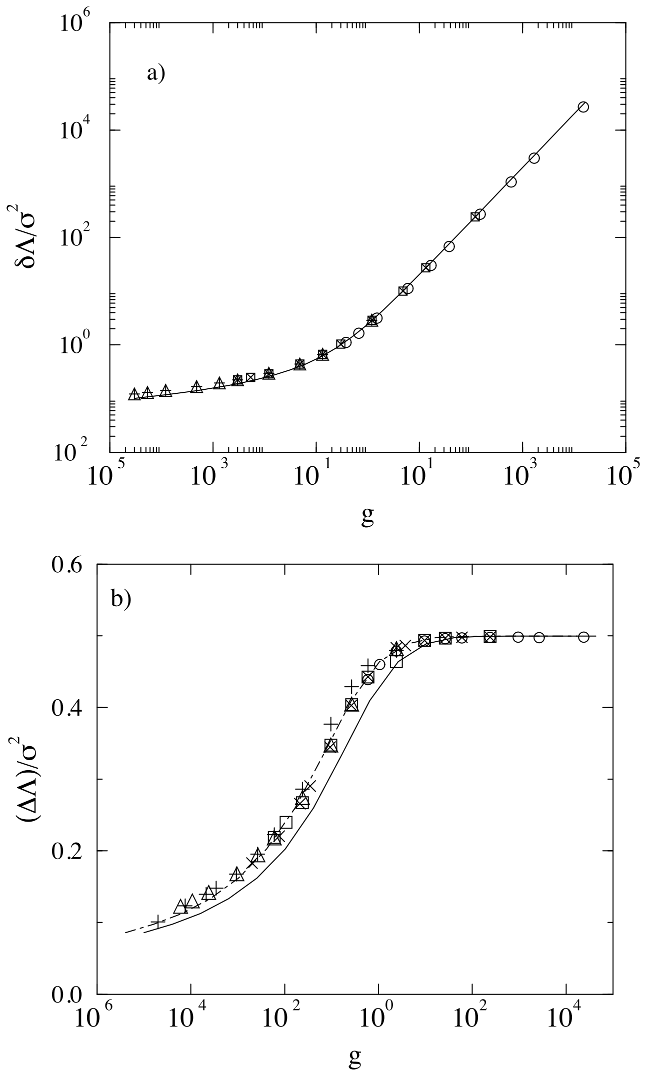

Figure 2. The Lyapunov exponent versus the scaling parameter g in the case of strictly positive multipliers. The data is obtained by varying ε, σ and for both choices of the probability distribution of the local multipliers (the cases (A) and (B) discussed in the text). In (*a*), the shift $\delta\lambda$ defined in equation (8) is reported, while in (*b*) the total shift $\Delta\Lambda$ (see equation (29)) is plotted. The solid curves correspond to the analytic expression. The dashed curve in (*b*) is the analytical curve arbitrarily shifted to show that a 'renormalization' of the scaling parameter could account for the remaining discrepancy with numerical data.

The data plotted this way are reported in figure 2(*b*). We clearly see that the trivial correction term -2γ cancels almost exactly the growth exhibited by $\delta\Lambda$ for large g values allowing for a more stringent test of the theoretical prediction. We can now see that the absolute difference is not larger than 0.05 and it could be greatly reduced by suitably shifting the theoretical curve (i.e. by rescaling g by approximately a factor of 2) as shown by looking at the dashed curve. However, in the absence of theoretical arguments, this observation cannot be considered as more than a hint for future considerations.

4. The general case

4.1. Theory

In this section, we also account for sign fluctuations. In order to keep the theoretical treatment as simple as possible, we shall assume that the sign is a δ-correlated stochastic process independent of the modulus, so that the average factorizes as

$$\langle m_i \rangle = (p - q)\langle |m_i| \rangle$$

where p (q) is the probability that m_i is positive (negative). The major difference with respect to the previous case is that the ratio R_i can also assume negative as well as positive values. It is therefore more convenient to work with R_i instead of introducing its logarithm which would require introducing absolute values and thus two different variables to account for the dynamics in the positive as well as in the negative range of R_i values.

In the previous section, we have seen that the coupling with the neighbouring sites compensate each other because of the symmetry $R \to 1/R$ ($w \to -w$). Accordingly, they have been neglected without causing much trouble to the theoretical approach. As the same symmetry is maintained in this case (besides the sign symmetry that was present before), we proceed in the same way, by neglecting the R_{i+1} and R_{i-1} terms in equation (10). At variance with the previous section, we have decided to introduce this approximation before expanding the dynamical rule in powers of γ. The reason is that, as we shall see, the latter step is more delicate in the present case and the crucial differences with the previous case can be better appreciated in the single-particle context. As a result one obtains,

$$R(t+1) = \mu(t)\frac{R(t) + \gamma}{1 + \gamma R(t)} \tag{30}$$

where, for the sake of simplicity, we have removed the now irrelevant site dependence. Mapping (30) possesses two remarkable symmetry properties: the evolution is invariant under the transformation $R \to 1/R$, since the stochastic process μ turns out to be invariant under the same transformation $\mu \to 1/\mu$ (it is sufficient to look at its definition). This is the same symmetry as that discovered in the previous section where we found that the potential $V(w)$ is an even function of w. As a consequence, we can restrict our analysis to the interval $[-1, 1]$.

The second symmetry has much more serious implications. We can see that the mapping (30) is also invariant under time reversal. More precisely, if we express $R(t)$ as a function of $R(t+1)$ we find the same functional form of mapping (30), provided that the change of variables $S : R(t+1) \to -R(t+1)/\mu(t)$ and $\mu \to 1/\mu$ are introduced as well. As the transformation S is an involution (i.e. $S^2 = Id$), we can state that mapping (30) is invariant under time reversal. Therefore, there seems to be a contradiction present, as this property also holds for strictly positive multipliers, when it is clear that there is an attractor (the point $w = 0$, i.e. $R = 1$), since time reversibility hints at a lack of attractors! Indeed, there is no contradiction, since time-reversal symmetry is broken in the case of strictly positive multipliers. In fact, invariance of the mapping only implies that a given solution can be neither stable nor unstable, if it is itself invariant under the involution S. However, this is not the case for the fixed point $R = 1$ (in the absence of noise, i.e. for $\mu = 1$) which is mapped by S onto $R = -1$, so that we can only conclude that if $R = 1$ is stable, then $R = -1$ must be unstable (as it is indeed the case). In other words, positive values of R are characterized by a contracting dynamics towards $R = 1$, while negative values depart from -1. If the multipliers are strictly positive, negative R values cannot be asymptotically observed as they lie in the repelling part of the phase space and the previous treatment in terms of a Langevin equation with an attracting force makes perfect sense. On the other hand, if the multipliers can assume both signs, the dynamical rule allows one to interchangeably visit the positive as well as the negative region. In principle, it is still possible to have, on average, a global contraction provided that a longer time is spent in the positive region. Actually, this is the assumption more or less implicitly made in [6], where it was conjectured that no qualitative changes are expected when positive and negative multipliers come into play except for the degenerate case $p = q = \frac{1}{2}$. We see below that even if the scaling behaviour in the limit of vanishing coupling is unaffected, this is not true and it indeed requires the introduction of a different scaling parameter.

The most effective way we have found to analyse mapping (30) is by exploiting another property: the possibility of transferring the change of sign of μ to γ. With this trick, the change of sign in equation (30) can be effectively treated perturbatively with γ being a small parameter. More precisely, if $\mu(t)$ happens to be negative, we can assume it to remain nevertheless positive and perform the next iteration with $-R(t+1)$. It can then be seen that the resulting expression is the same as the original one after changing the sign of γ and $\mu(t+1)$. Now, irrespective of the sign of $-\mu(t+1)$, we assume it to be positive and transfer its sign to the next value of γ. In other words, we can iterate the mapping

$$R(t+1) = |\mu(t)| \frac{R(t) + \gamma(t)}{1 + \gamma(t)R(t)} \tag{31}$$

where the sign of $\gamma(t)$ is that of $\prod_{s=1}^{t-1} \mu(s)$. We can immediately see that even if μ is, on average, more positive than negative (or vice versa), the sign of γ has no preference, since it simply depends on the parity of the number of sign changes. It is due to this reason that fluctuating multipliers are qualitatively different from strictly positive ones: even an asymmetry in the signs (a preference, say, for the positive values) implies that the unstable and stable regions (positive and negative values of R in the initial representation) are equally visited.

The dichotomous structure of the noise $\gamma(t)$ allows one to express the stochastic map as the sum of a net drift plus a zero-average fluctuating term. Indeed, by calling $F_+(R)$ and $F_-(R)$ the lhs of equation (31) whenever γ is positive, or respectively, negative, we can write

$$R(t+1) = \frac{1}{2}\{F_+(R(t)) + F_-(R(t))\} + \frac{\delta(t)}{2}\{F_+(R(t)) - F_-(R(t))\} \tag{32}$$

where $\delta(t)$ is again a dichotomous noise with entries equal to ± 1. More specifically,

$$R(t+1) = |\mu| \frac{(1-\gamma^2)R}{1-\gamma^2 R^2} + |\mu|\delta(t) \frac{\gamma(1-R^2)}{1-\gamma^2 R^2}. \tag{33}$$

In order to obtain an analytic expression for the probability density of R, it is convenient to turn this equation into a continuous-time model. Proceeding step by step, let us first expand in powers of γ and retain contributions up to second order,

$$R(t+1) = |\mu|[1 - \gamma^2(1-R^2)]R + |\mu|\delta(t)\gamma(1-R^2). \tag{34}$$

Let us now assume that the fluctuations of $|\mu|$ are small, i.e. we write $|\mu| = 1+\nu+\overline{\nu}$, where both ν and $\overline{\nu}$ are small compared with one and the average $\langle\nu\rangle = 0$. From the equality $\langle\log\mu\rangle = 0$ (see the definition equation (11)) it is immediately seen that, up to leading order,

$$\overline{\nu} = \overline{\sigma}^2/2 \tag{35}$$

where $\overline{\sigma}^2$ is the variance of ν. After substituting $|\mu| = 1 + \nu + \overline{\sigma}^2/2$ in equation (34) and neglecting higher-order contributions, we obtain

$$\dot{R} = \gamma^2(R^2-1)R + (\nu + \overline{\sigma}^2/2)R + \delta(t)\gamma(1-R^2) \tag{36}$$

where $\dot{R}$ is defined as $R(t+1) - R(t)$. Notice that the above stochastic equation must be interpreted in the Ito sense as it follows from a discrete-time process.

It is now very instructive to compare this stochastic process with the one discussed in the previous section, where no sign fluctuations have been considered. Assuming no sign fluctuations is tantamount to setting $\delta(t) = 1$. As a result, the last term in the rhs of equation (36) corresponds to a drift process. Additionally, it is much larger than the first contribution which can thus be neglected,

$$\dot{R} = \gamma(1 - R^2) + (\nu + \overline{\sigma}^2/2)R. \tag{37}$$

A straightforward application of the Ito calculus (see, e.g., [22]), shows that the above equation is equivalent to equation (21). For those who are not familiar with this kind of transformation, we briefly sketch an equivalent and more transparent derivation. Let us return to the discrete time representation (i.e. replace $\dot{R}$ with $R(t+1) - R(t)$) and once again introduce the variable $w = \ln R$. We obtain,

$$w(t+1) = w(t) + \log\{1 + \gamma(\mathrm{e}^{-w} - \mathrm{e}^{w}) + \nu + \overline{\sigma}^2/2\}. \tag{38}$$

By expanding the logarithm and including the only relevant quadratic term proportional to ν^2 (the average of which exactly compensates the last term $\overline{\sigma}^2/2$), we arrive precisely at the discretized version of equation (21). The only irrelevant difference is that ξ is now equal to ν instead of $\ln\mu$ (the two quantities coincide in the small noise limit). As a consequence, the present derivation is perfectly consistent with the results discussed in the previous section.

Let us now return to the general expression (36). If the time variable is rescaled by a factor $\overline{\sigma}^2$, it is immediately recognized that the dynamics of R depends on just one parameter

$$G = \frac{\gamma}{\overline{\sigma}} \tag{39}$$

which is again a ratio between coupling strength and multiplier fluctuations. However, there is an important difference with the parameter $g = \gamma/\sigma^2$ introduced in the previous case, as it is seen by noticing that in the small $\overline{\sigma}$ limit, the equality

$$\overline{\sigma} = \sqrt{2}\sigma \tag{40}$$

holds. Apart from the irrelevant numerical factor, it turns out that, in the general case, the rms rather than the standard deviation enters as a measure of multiplier fluctuations.

According to the Ito interpretation of the stochastic differential equation (36), the Fokker–Planck equation reads, in rescaled time units, as

$$\frac{\partial P}{\partial t} = -\frac{\partial}{\partial R}(AP) + \frac{1}{2}\frac{\partial^2}{\partial R^2}(BP) \tag{41}$$

where

$$A(R) = -G^2 R(1 - R^2) + R/2 \tag{42}$$

is the drift term, while

$$B(R) = R^2 + G^2(1 - R^2)^2 \tag{43}$$

is the diffusion coefficient. Since $4A(R) = \mathrm{d}B/\mathrm{d}R$, the stationary solution is

$$P(R) = \frac{N(G)}{\sqrt{G^2(1 - R^2)^2 + R^2}} \tag{44}$$

where $N(G)$ is the normalization constant discussed in appendix B.

An expression for the Lyapunov exponent can be obtained from equation (8), by integrating over the above-determined probability distribution. Unfortunately, there is a crucial difference with the previous case: we cannot simply expand the logarithm in powers of γ, since this leads to computing the first moment of $P(R)$ which is already a diverging quantity ($P(R)$ decays

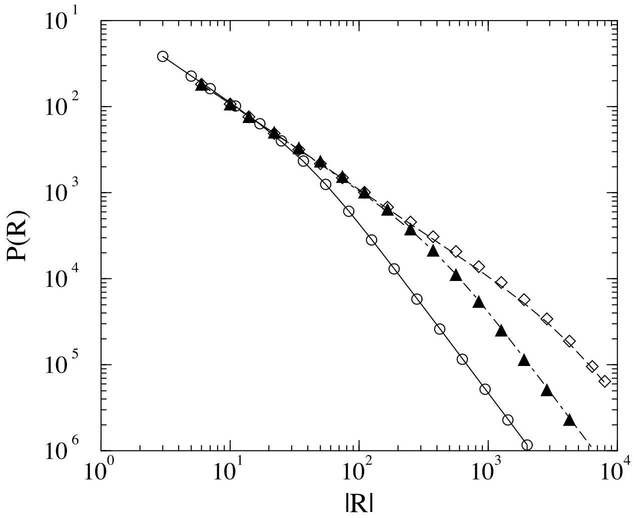

Figure 3. Log–log plot of the probability distribution $P(R)$ to highlight the power-law behaviour. Circles, triangles and diamonds refer to $G = \sqrt{6} \times 10^{-2}$, $\sqrt{6} \times 10^{-3}$, $\sqrt{6} \times 10^{-5}$, respectively. The simulation details are as in figure 1. The various curves represent the analytical results as from equation (44).

to zero as slowly as $1/R^2$). Obviously, this is only a numerical artifact: the average of the logarithm itself is still well defined and has a finite value.

Nevertheless, this is an indication that we must be much more cautious in performing power expansions. In particular, this difficulty prevents one from obtaining a general analytical expression analogous to that obtained in the previous section in terms of modified Bessel functions. In this case, even obtaining an expression in the limiting case of small G requires rather laborious work. In appendix B we illustrate that one can eventually show that the non-trivial deviation with respect to the uncoupled limit is given by

$$\delta\Lambda = \frac{3\sigma^2}{2\ln(1/G)}. \tag{45}$$

Therefore, we also see that in the general case of positive/negative signs, the leading dependence on ε is of the type $1/\ln\varepsilon$, as numerically observed. What is different is the dependence on the multiplier fluctuations as testified by the presence of the parameter G rather than g.

4.2. Numerical results

The first meaningful test of the analytical approach devised in section 4 concerns the probability distribution $P(R)$. In figure 3 we report the outcome of a numerical experiment in doubly logarithmic scales (see the various symbols). This allows one to observe a crossover from an initial decay as $1/R$ to the asymptotic decay $1/R^2$, which represents the first qualitative confirmation of the theoretical predictions. However, the agreement with expression (44) (represented by the various lines) is more than just qualitative. In fact, besides noticing the almost perfect overlap, one should also remember that the only parameter entering equation (44), i.e. G, has not been fitted, but independently determined from the fluctuations of the local multipliers. As a last remark, we would like to point out that the good agreement is not totally obvious *a priori* at least for the reason that the reduction from a set of coupled stochastic equations to a single equation is not completely under control.

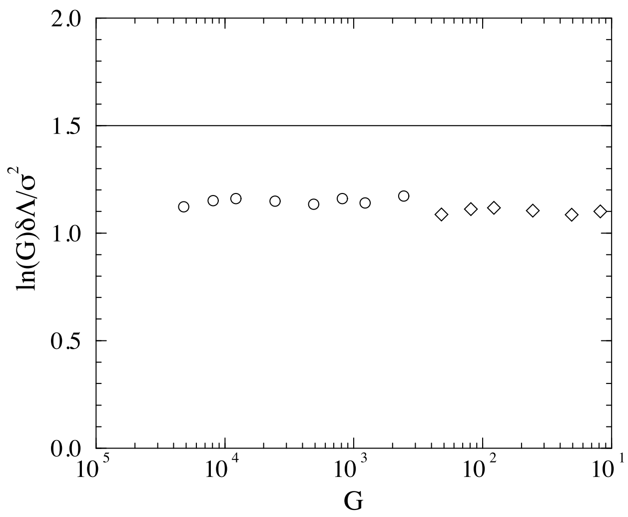

Figure 4. The Lyapunov exponent versus the scaling parameter G in the case of fluctuating multipliers. The Lyapunov correction $\delta\Lambda$ is normalized so as to emphasize the $1/|\ln G|$ dependence. Circles correspond to $\varepsilon = 10^{-5}$ while diamonds to $\varepsilon = 10^{-3}$. The solid line represents the theoretical result (45).

Moreover, it is instructive to compare the shape of this distribution with the results predicted by the theory for strictly positive multipliers. By expressing the probability density of equation (22) in terms of R, we find an exponential tail ($P(R) \simeq \exp(-gR)/R$). The power law observed in figure 3 is also, therefore, evidence of a clear difference between the two regimes.

Finally, let us look at the deviations of the MLE plotted versus the scaling parameter G. The data reported in figure 4 have been obtained for different noise amplitudes and either $\varepsilon = 10^{-3}$ (diamonds) or $\varepsilon = 10^{-5}$ (circles). It is clearly seen that, $\delta\Lambda \ln G/\sigma^2$ is constant, and independent of the value of G. This confirms the scaling behaviour predicted by equation (45). A more quantitative check can be made by comparing the actual value of $\delta\Lambda \ln G/\sigma^2$ (about $1.1 \approx 1.2$ in direct simulations) with the theoretical prediction (1.5). We believe that the deviation can be ascribed to the approximation made in reducing the set of coupled stochastic equations to a single Langevin equation.

5. Conclusions and perspectives

In this paper we have developed a theoretical method that is able to explain the scaling behaviour of the MLE previously observed in CMLs in the small-coupling limit [7]. Furthermore, our treatment provides a quantitative estimation although under the assumption of δ-correlated multipliers (i.e. in the random matrix approximation). It is important to stress that such quantitative results have been obtained not only in the case of strictly positive multipliers (the only one dealt with in the previous studies) but also in the case of random signs.

In both cases we have found that the correction to the MLE induced by the local interactions actually depends on a single scaling parameter which is simply the coupling strength rescaled by the 'amplitude' of multiplier fluctuations. However, the scaling parameter is significantly different in the two cases: for strictly positive multipliers, the fluctuation 'amplitude' is the mean-square deviation σ^2 (see the definition of g—equation (18)), while in the case of random signs, the 'amplitude' is the rms deviation (see the definition of G—equation (39)). Important differences affect also the probability distribution of the ratios R_i of the perturbation amplitude in two adjacent sites: in the case of fluctuating signs, long tails characterized by a power-law decay are present.

Among the problems still open, there is certainly the exigency of a more rigorous procedure to solve the set of coupled Langevin equations. In fact, while the derivation of the set of coupled stochastic equations is the result of a well controlled perturbative approach, its reduction to a single equation is based on a mean-field approximation whose validity cannot be controlled *a priori* but only checked *a posteriori*.

As the analytic formulae provide a good description of the ideal random-matrix case, it would be now interesting to compare our predictions with the actual evolution of a generic CML and if possible take care of modifications of the invariant measure as well as of the temporal correlations.

Finally, we want to mention the possibility of extending this approach to the case of weakly coupled attractors, where time is continuous from the very beginning. This is certainly the most stimulating perspective that is also supported by the preliminary observation that the Langevin equation (21) is also obtained in the case of two weakly coupled differential equations [16].

Acknowledgments

We thank the Institute of Scientific Interchange (ISI) in Torino, Italy, where this work was started and partly carried on. We are also indebted to J M Parrondo for having pointed out the opportunity to adopt the Ito interpretation.

Appendix A. Linear limit

This appendix is devoted to the analysis of equation (15) in the linear limit,

$$\dot{w}_i = -\gamma(w_{i+1} - 2w_i + w_{i-1}) + \psi_i(t) - \psi_{i-1}(t) \tag{A1}$$

where we have introduced $\psi_k = \ln\{m_k(t)\}$. This is apparently a discretized Edwards–Wilkinson equation [23], but the spatial structure of the noise prevents the onset of any roughening phenomenon (as commented in the main body of the paper).

To solve this equation, it is convenient to perform a spatial Fourier transform, since it leads to a set of uncoupled equations,

$$\dot{w}(k, t) = -2\gamma(1 - \cos(k))w(k, t) + (1 - \mathrm{e}^{\mathrm{i}k})\psi(k, t) \tag{A2}$$

where $w(k, t)$ is a complex number that can be decomposed into a real and imaginary part ($w(k, t) = x(k, t) + \mathrm{i}y(k, t)$), which satisfy the same equation

$$\dot{x}(k, t) = -2\gamma(1 - \cos(k))x(k, t) + \eta(k, t) \tag{A3}$$

where the noise term η is δ correlated,

$$\langle \eta(t)\eta(t')\rangle = 2\sigma^2(1 - \cos(k))\delta(t - t'). \tag{A4}$$

Accordingly, all Fourier modes obey the same Gaussian distribution function,

$$P\{w\} \sim \exp\left(-\frac{\gamma(x^2 + y^2)}{2\sigma^2}\right). \tag{A5}$$

The probability distribution of w_i on a single site is easily obtained by summing the independent distributions corresponding to all modes. As a result, the distribution of w_i is also Gaussian and its variance is σ^2, as if we had neglected the spatial coupling in equation (A1).

Appendix B. Lyapunov correction

In this appendix we determine the nontrivial part of the leading correction to the MLE in the general case. We start by computing the normalization constant. It is convenient to exploit the invariance of $P(R)$ under parity change and the transformation $R \to 1/R$, to express the normalization condition as

$$1 = 4\int_0^1 \mathrm{d}R\, P(R) = 4N(G)\int_0^1 \frac{\mathrm{d}R}{\sqrt{R^2 + G^2(1-R^2)^2}}. \tag{B1}$$

Since an explicit analytical expression for the above integral does not exist, we shall limit ourselves to studying the small-G limit. One cannot simply expand the denominator, as it gives rise to a non-integrable singularity in $R = 0$. It is, instead, convenient to introduce the variable $x = R/G$. Afterwards, one can expand the integrand in powers of G without encountering undesired divergences. By retaining the leading terms, we find

$$\frac{1}{N} \simeq 4\int_0^{1/G} \frac{\mathrm{d}x}{\sqrt{1+x^2}} \simeq 4\ln(1/G). \tag{B2}$$

From equations (7), (5), it turns out that the estimation of $\delta\Lambda$ requires computing the mean value of $L(R_1, R_2) \equiv \ln|1 + \gamma R_1 + \gamma/R_2|$, i.e.

$$\delta\Lambda = \int_{-\infty}^{\infty}\int_{-\infty}^{\infty} \mathrm{d}R_1\,\mathrm{d}R_2\, P(R_1)P(R_2)L(R_1, R_2). \tag{B3}$$

Thanks to the equality $L(R_1, R_2) = L(1/R_2, 1/R_1)$ and to the invariance of $P(R)$ under the transformation $R \to 1/R$, we can write the Lyapunov correction as the sum of three different contributions, namely

$$\begin{aligned}\delta\Lambda \equiv \delta_1 + \delta_2 + \delta_3 = \int_{-1}^{1}\int_{-1}^{1} \mathrm{d}R_1\,\mathrm{d}R_2\, P(R_1)P(R_2)\{L(R_1, 1/R_2)\\ +2L(R_1, R_2) + L(1/R_1, R_2)\}\end{aligned} \tag{B4}$$

where the meaning of the new symbols is obvious.

In analogy with the computation of the normalization constant, we introduce the variables $x = R_1/G$ and $y = R_2/G$. As a consequence, the expressions for the three contributions can be written as

$$\delta_1 = N^2\int_{-1/G}^{1/G}\int_{-1/G}^{1/G} \mathrm{d}x\,\mathrm{d}y\, \frac{\ln|1 + \gamma Gx + \gamma Gy|}{\sqrt{x^2 + (1-G^2x^2)^2}\sqrt{y^2 + (1-G^2y^2)^2}} \tag{B5}$$

$$\delta_2 = 2N^2\int_{-1/G}^{1/G}\int_{1/G}^{1/G} \mathrm{d}x\,\mathrm{d}y\, \frac{\ln|1 + \gamma Gx + \gamma/(Gy)|}{\sqrt{x^2 + (1-G^2x^2)^2}\sqrt{y^2 + (1-G^2y^2)^2}} \tag{B6}$$

$$\delta_3 = N^2\int_{-1/G}^{1/G}\int_{-1/G}^{1/G} \mathrm{d}x\,\mathrm{d}y\, \frac{\ln|1 + \gamma/(Gx) + \gamma/(Gy)|}{\sqrt{x^2 + (1-G^2x^2)^2}\sqrt{y^2 + (1-G^2y^2)^2}}. \tag{B7}$$

The inequalities $\gamma \ll G \ll 1$ imply that the contributions proportional to γG in the arguments of the logarithms can be neglected so that δ_1 is altogether negligible. Moreover, G can be always neglected in the denominators, so that the leading contribution to the MLE can be determined by merely estimating the two integrals

$$\delta_2 = 2N\int_{-1/G}^{1/G} \mathrm{d}y\, \frac{\ln|1 + \overline{\sigma}/y|}{\sqrt{1+y^2}} \tag{B8}$$

$$\delta_3 = N^2\int_{-1/G}^{1/G}\int_{-1/G}^{1/G} \mathrm{d}x\,\mathrm{d}y\, \frac{\ln|1 + \overline{\sigma}/x + \overline{\sigma}/y|}{\sqrt{1+x^2}\sqrt{1+y^2}} \tag{B9}$$

where we have re-introduced the parameter $\overline{\sigma}$ for later convenience. We start by discussing δ_2; it cannot be computed by expanding the logarithm as this leads to an unphysical divergence. It is, instead, helpful to split this contribution into two parts

$$\begin{aligned}\delta_2 &= \delta_2' + \delta_2'' \\ &= 2N\int_{-1/G}^{1/G} \mathrm{d}y\, \frac{\ln|y+\overline{\sigma}|}{\sqrt{1+y^2}} - 2N\int_{-1/G}^{1/G} \mathrm{d}y\, \frac{\ln|y|}{\sqrt{1+y^2}}.\end{aligned} \tag{B10}$$

The first integral can be estimated by introducing the variable $w = y+\overline{\sigma}$ and thereby expanding the denominator in powers of $\overline{\sigma}$. By retaining terms up to the second order, we find that δ_2' can be written as

$$\delta_2' = 2N\int_{-1/G+\overline{\sigma}}^{1/G+\overline{\sigma}} \mathrm{d}w\, \left\{\frac{\ln|w|}{\sqrt{1+w^2}} + \overline{\sigma}\frac{w\ln|w|}{(1+w^2)^{3/2}} + \frac{\overline{\sigma}^2}{2}\frac{w^2\ln|w|}{(1+w^2)^{5/2}}(2w^2-1)\right\}. \tag{B11}$$

By expanding the zeroth-order term around the integral boundaries in powers of $\overline{\sigma}$, we find that it is equal to $-\delta_2''$ plus corrections of the order $\gamma^2 \ln G$. A contribution of the same order is obtained also by integrating the linear term in $\overline{\sigma}$. However, the leading contribution to the MLE comes from the second-order term which, in the small-G limit can be written as

$$\delta_2 = 2N\overline{\sigma}^2 \int_0^\infty \mathrm{d}w\, \frac{\ln w}{(1+w^2)^{5/2}}(2w^2-1). \tag{B12}$$

The integral can be analytically solved and turns out to be equal to one, so that†

$$\delta_2 = 2N(G)\overline{\sigma}^2 = \frac{\overline{\sigma}^2}{2\ln(1/G)}. \tag{B13}$$

In principle, the determination of δ_3 requires even more cumbersome calculations, as it involves a double integral. However, formally deriving the expression for δ_3/N^2 with respect to G, we find that, up to negligible corrections,

$$\frac{\mathrm{d}\delta_3/N^2}{\mathrm{d}G} = -\frac{4}{G}\int_{-1/G}^{1/G} \mathrm{d}y\, \frac{\ln|1+\overline{\sigma}/y|}{\sqrt{1+y^2}}. \tag{B14}$$

As the integral in this expression is exactly the same as that involved in the definition of δ_2 (see equation (B8)), we can write

$$\frac{\mathrm{d}\delta_3/N^2}{\mathrm{d}G} = -\frac{2\delta_2}{GN}. \tag{B15}$$

Upon substituting the expression for δ_2 (see equation (B13)), the above equations can be rewritten as

$$\frac{\mathrm{d}\delta_3/N^2}{\mathrm{d}G} = -\frac{4\overline{\sigma}^2}{G} \tag{B16}$$

which, after integration, yields

$$\delta_3 = \frac{\overline{\sigma}^2}{4\ln(1/G)}. \tag{B17}$$

In conclusion, we find that

$$\delta\Lambda = \frac{3\sigma^2}{2\ln(1/G)} \tag{B18}$$

where we have preferrentially introduced the explicit dependence on the physical parameter σ rather than $\overline{\sigma}$.

† We have solved it with the help of the Maple software package.

References

[1] Bunimovich L and Sinai Ya 1988 *Nonlinearity* **1** 491
[2] Aubry S and MacKay R S 1994 *Nonlinearity* **7** 1623
[3] Rosenblum M G, Pikovski A S and Kurths J 1997 *Phys. Rev. Lett.* **78** 4193 and references therein
[4] Daido H 1984 *Prog. Theor. Phys.* **79** 75
Daido H 1985 *Phys. Lett.* A **110** 5
[5] Yang W, Ding E-J and Ding M 1996 *Phys. Rev. Lett.* **76** 1808
[6] Torcini A, Livi R, Politi A and Ruffo S 1997 *Phys. Rev. Lett.* **78** 1391
[7] Livi R, Ruffo S and Politi A 1992 *J. Phys. A: Math. Gen.* **25** 4813
[8] Paladin G and Vulpiani A 1986 *J. Phys. A: Math. Gen.* **19** 1881
[9] Parisi G and Vulpiani A 1986 *J. Phys. A: Math. Gen.* **19** L425
[10] Derrida B and Gardner E 1984 *J. Physique* **45** 1283
[11] Cecconi F and Politi A 1997 *Phys. Rev.* E **56** 4998
[12] Derrida B and Spohn H 1988 *J. Stat. Phys.* **51** 817
[13] Cook J and Derrida B 1989 *Europhys. Lett.* **10** 195
Cook J and Derrida B 1990 *J. Phys. A: Math. Gen.* **23** 1523
Cook J and Derrida B 1990 *J. Stat. Phys.* **61** 961
[14] Pikovsky A S and Kurths J 1994 *Phys. Rev.* E **49** 898
[15] Pikovsky A S and Politi A 1994 *Nonlinearity* **11** 1049
[16] Pikovsky A 1999 Private communication
[17] Gradshteyn I S and Ryzhik I M 1965 *Table of Integrals, Series and Products* (New York: Academic)
[18] Abramowitz M and Stegun I A *Handbook of Mathematical Functions* (New York: Dover)
[19] Cecconi F 1999 *PhD Thesis*
[20] Benettin G, Galgani L, Giorgilli A and Strelcyn J-M 1980 *Meccanica* **9** 21
Shimada I and Nagashima T 1979 *Prog. Theor. Phys.* **61** 1605
[21] Isola S, Politi A, Ruffo S and Torcini A 1990 *Phys. Lett.* A **143** 365
[22] Gardiner C W 1985 *Handbook of Stochastic Methods* (Berlin: Springer)
[23] Barábasi A-L and Stanley H E 1995 *Fractal Concepts in Surface Growth* (Cambridge: Cambridge University Press)